Journal of Solid State Chemistry 184 (2011) 405–410

Contents lists available at ScienceDirect

Journal of Solid State Chemistry

journal homepage: www.elsevier.com/locate/jssc

Fluorine sites in glasses and transparent glass-ceramics of the system $Na_2O/K_2O/Al_2O_3/SiO_2/BaF_2$

Christian Bocker [a,*], Francisco Muñoz [b], Alicia Durán [b], Christian Rüssel [a]

[a] Otto-Schott-Institut, Jena University, Fraunhoferstr. 6, 07743 Jena, Germany
[b] Instituto de Cerámica y Vidrio (CSIC), Kelsen 5, 28049 Madrid, Spain

ARTICLE INFO

Article history:
Received 2 September 2010
Received in revised form
17 November 2010
Accepted 1 December 2010
Available online 7 December 2010

Keywords:
NMR
Crystal growth
Crystallization
Nano crystals
Silicate glasses

ABSTRACT

The transparent glass-ceramics obtained in the silicate system $Na_2O/K_2O/SiO_2/BaF_2$ show homogeneously dispersed BaF_2 nano crystals with a narrow size distribution. The X-ray diffraction and the nuclear magnetic resonance spectroscopy were applied to glasses and the respective glass-ceramics in order to clarify the crystallization mechanism and the role of fluorine during crystallization. With an increasing annealing time, the concentration and also the number of crystals remain approximately constant. With an increasing annealing temperature, the crystalline fraction increases until a saturation limit is reached, while the number of crystals decreases and the size of the crystals increases. Fluoride in the glassy network occurs as Al–F–Ba, Al–F–Na and also as Ba–F structures. The latter are transformed into crystalline BaF_2 and fluoride is removed from the Al–F–Ba/Na bonds. However, some fluorine is still present in the glassy phase after the crystallization.

1. Introduction

Glass-ceramics containing fluoride crystallites are valuable materials for photonic applications. Especially, alkaline earth fluoride crystals are known as good host materials for rare earth ions such as Er^{3+} or Eu^{3+} [1–3]. These doped glass-ceramics are advantageous for some applications, because they can be easily processed by the viscous flow, e.g. drawn to a fiber. After subsequent annealing and crystallization of the glasses, optical properties, e.g. fluorescence lifetimes and luminescence or up-conversion efficiencies [4–6]. These materials might be used, for example, as optical amplifiers or in fiber lasers [7,8]. In order to obtain transparent glass-ceramics i.e. to avoid light scattering, the size of the crystals must be much smaller than half of the wavelength of the used light.

The formation of nano crystals in a multi-component glass system containing BaF_2 or CaF_2 was recently explained by the formation of a diffusion barrier around the forming crystals [9–11]. The nano crystals were homogeneously distributed within the glass matrix and possessed a narrow crystallite size distribution [12]. When in multi-component glasses, a metal fluoride component is crystallized, a layer around the crystal is depleted in the respective components. Since in the case of metal fluorides, these compounds act as the network modifying component; this leads to an enrichment in network formers, and hence increases the viscosity. This layer might act as a diffusion barrier and hinders further crystal growth [13,14].

The role of fluorine in aluminosilicate glass networks was studied by several researchers [15–19]. By means of solid-state nuclear magnetic resonance (NMR), it is possible to study the local environment of the involved atoms in the crystallization process. An NMR of fluorine-containing aluminosilicate glasses has shown that fluorine atoms are preferentially coordinated to aluminium instead of silicon, due to their tendency to bond with small and highly charged cations [19]. Generally, the larger the ionic field strength of the modifier cations, the higher is their ability to form chemical bonds to fluorine [20].

In this paper, a study on the BaF_2 concentration and the incorporation of fluorine during the course of BaF_2 crystallization in glass-ceramics in the system $Na_2O/K_2O/Al_2O_3/SiO_2/BaF_2$ through X-ray diffraction (XRD) and NMR is reported.

2. Experimental procedures

Glasses with the compositions $(100-x)(2Na_2O \cdot 16K_2O \cdot 8Al_2O_3 \cdot 74SiO_2) \cdot xBaF_2$ (in mol%), with $x=0$, 1, 2, 3, 4, 5 and 6, were melted from reagent grade Na_2CO_3, K_2CO_3, BaF_2, $Al(OH)_3$ and SiO_2 (quartz) in batches of 200 g. The covered platinum crucible was placed in a furnace at 1590 °C and kept for 1.5 h. The melts were cast onto a copper block and were subsequently put into a furnace preheated to 450 °C. Then the furnace was switched off and the glass was allowed to cool to room temperature. During melting, fluorine is

* Corresponding author. Fax: +49 3641 948502.
E-mail address: christian.bocker@uni-jena.de (C. Bocker).

0022-4596/$ - see front matter © 2010 Elsevier Inc. All rights reserved.
doi:10.1016/j.jssc.2010.12.001

lost due to an unavoidable evaporation. The fluorine concentration was determined by a wet-chemical method [21], X-ray fluorescence and energy-dispersive X-ray spectrometry. On the average about (34 ± 3)% of fluorine was lost during melting. Wet chemical analyses and energy-dispersive X-ray spectrometry were in good agreement (± 10%).

The glasses with 6 mol% BaF_2 were annealed at temperatures in the range 500–600 °C, for 20 h. For the samples annealed at 500 and 540 °C, the annealing time was varied in the range 5–160 h. The X-ray diffraction (XRD) patterns were recorded from powdered samples, using a Siemens D5000 diffractometer. To quantitatively determine the fraction of the crystalline BaF_2, the method of Rietveld-refinement was applied to the obtained XRD-patterns. An internal standard (25 wt% Al_2O_3) was added to the powdered samples [22].

^{19}F magic angle spinning (MAS) nuclear magnetic resonance (NMR) spectra were recorded with a Bruker ASX 400 spectrometer operating at 376 MHz (9.4 T), using a 2.5 mm probe. The pulse time was 1 μs and 30 s recycling time and 4.5 μs death time were used. A total number of 300 scans were accumulated with a spinning rate of 25 kHz. The background signal from the probe was registered for an empty rotor under the same conditions and removed from the ^{19}F spectra of all samples. Solid CaF_2 was used as the secondary reference with a chemical shift of −0.108 ppm with respect to $CFCl_3$ reference.

^{27}Al MAS NMR spectra were recorded with a Bruker ASX 400 spectrometer operating at 104.27 MHz (9.4 T), using a 4 mm probe. The pulse time used was 2.7 μs and the recycling time 2 s with 6 μs death time. A total number of 1024 scans was accumulated with a spinning rate of 10 kHz and as the chemical shift reference $AlCl_3 \cdot 6H_2O$ was used.

3. Results

The obtained glasses and glass-ceramics were all colorless and transparent. Fig. 1 shows the XRD-patterns of the glass and glass-ceramic samples obtained after annealing at 500 and 600 °C for 20 h, and at 500 °C for 160 h. The glass sample was amorphous while after annealing at 500 °C for 20 h broadened resonance peaks appeared. The mean crystallite sizes of the samples annealed at 500 °C were approximately 7 nm, as calculated by using Rietveld-refinement. Although the peaks of the sample, annealed for 160 h at 500 °C, seem broader in Fig. 1, the values are within an assumed accuracy of ± 0.5 nm. For the sample annealed at 600 °C for 20 h, a mean crystallite size of 15 nm was calculated. All peaks were attributable to the crystalline cubic BaF_2 (JCPDS no. 4-452).

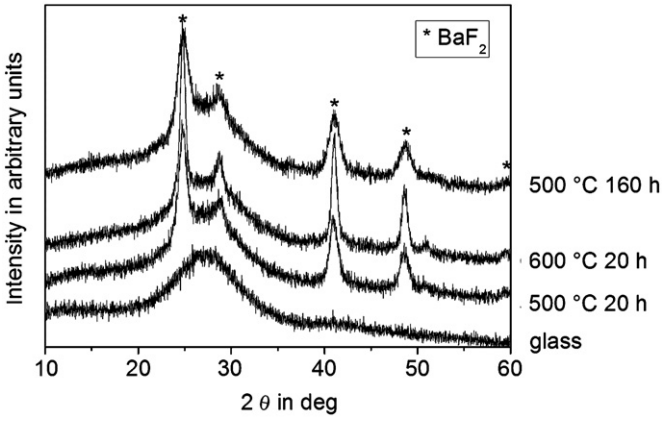

Fig. 1. XRD-patterns of the glass with the composition $1.9Na_2O \cdot 15K_2O \cdot 7.5Al_2O_3 \cdot 69.6SiO_2 \cdot 6BaF_2$ (in mol%) and of the samples annealed at 500 and 600 °C for 20 h and annealed at 500 °C for 160 h.

Annealing at a temperature of 500 °C for 160 h did not lead to the formation of any additional crystalline phase.

Fig. 2 shows the quantity of crystalline BaF_2, as a function of annealing time, at 500 and 540 °C. After annealing the sample for 2 h at 500 °C, approximately 2 wt% of BaF_2 is precipitated. After annealing for 160 h, the concentration of crystalline BaF_2 increases to about 5 wt%. Annealing the sample at 540 °C for 20 h resulted in the crystalline BaF_2 with a concentration of 5 wt%. Annealing for 40 h, results in an increase in the BaF_2 concentration to about 6 wt%. A further increase in the BaF_2 concentration is not observed within the limits of an error, if the sample is annealed for 80 h at 540 °C.

Fig. 3 shows a plot of the quantity of crystalline BaF_2 as a function of temperature at a constant annealing time of 20 h. With an increasing annealing temperature, the concentration increases slightly from approximately 4 wt% at 500 °C up to about 5 wt% at 520 °C and is not changing within the limits of error, while further increasing the temperature to 600 °C.

Fig. 4 shows the ^{19}F Magic Angle Spinning (MAS) NMR spectra of the oxyfluoride glass and glass-ceramics obtained by annealing at

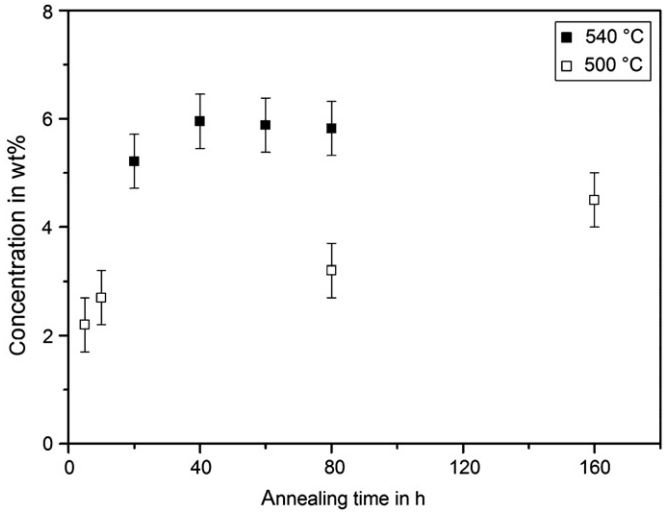

Fig. 2. Quantity of crystalline BaF_2 in wt% calculated by Rietveld-refinement from XRD-patterns of samples annealed at 500 °C (open square symbols) and 540 °C (full square symbols) as a function of annealing time.

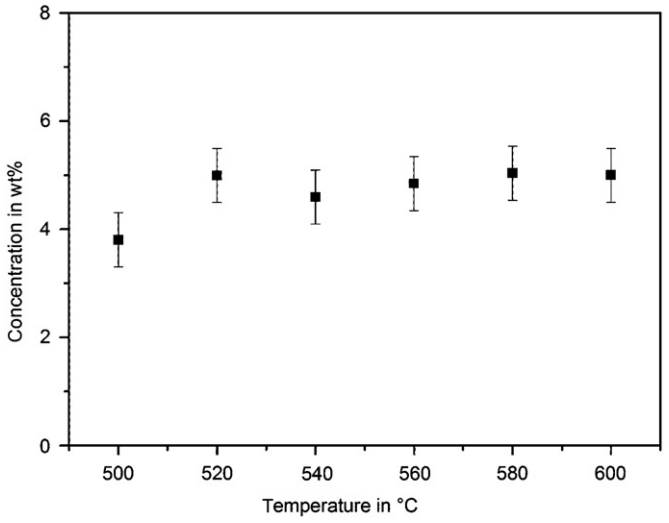

Fig. 3. Quantity of crystalline BaF_2 in wt% calculated by Rietveld-refinement from XRD-patterns of the glass-ceramics annealed for 20 h as a function of annealing temperature.

temperatures in the range 500–600 °C for 20 h. The spectrum of the base glass presents a resonance band with a maximum in the range −174 to −173 ppm, and a second very broad band with a maximum centered at around −140 ppm. Due to their width, it is not possible to deduce how many bands exactly contribute to these resonances. According to Kiczenski et al. [16], the resonances at a precise chemical shift of −173 ppm should be attributed to fluorine atoms within an Al–F–Al environment. However, it is not possible to exclude other possibilities such as Al–F–Al(Na^+) structures reported to occur at −166 ppm; Al–F–Al(Ba^+) structures which should appear at −155.6, −145.9 or −150.1 and −140 ppm; and Al–F–K at −155 ppm or Al–F–Na structures which should be observed between −190 and −180 ppm [16]. The broad resonance found in all glass-ceramics in the range −160 to −100 ppm, with a maximum at approximately −140 ppm, may be caused by different structures in which fluorine atoms coordinated with aluminium and additionally with Ba^{2+} or Na^+ cations. Furthermore, a very small and also broad resonance is detected within the range −25 to 50 ppm which, according to the literature [20], should be attributed to fluorine in Ba–F clusters within an amorphous structure.

The ^{19}F MAS NMR spectra of the glass-ceramic samples again show the two previously mentioned resonances with the maxima centered at −180 and −140 ppm. Both are very broad and show much smaller intensities. Additionally, a very strong resonance centered at −16 ppm appears, which is assigned to fluorine in the crystalline BaF_2 [16]. A deconvolution of the resonance band centered at −16 ppm, including spinning side bands, has been carried out by using DMFIT software [23]. Table 1 summarizes the results of the deconvolution procedure for the ^{19}F signal related to fluorine atoms in the crystalline BaF_2. It is seen that 35% of fluorine in the glass is already incorporated into the crystalline phase after annealing the sample at 500 °C for 20 h. Annealing at higher temperatures gives rise to a small increase in the concentration of fluorine atoms incorporated into the crystals. All other fluorine atoms seem to be incorporated in Al–F–Na or Al–F–Ba structures in the same manner as in the base glass. It is already shown in Fig. 3 that for a constant annealing time of 20 h, the BaF_2 concentration is smaller after annealing at 500 °C and remains constant within the limits of an error for annealing temperatures in the range 520–600 °C.

Finally, it is worth noting that other small resonances can be seen within the NMR spectra of the glass-ceramic samples, whose centers are at 7, −40 and −67 ppm, which unfortunately are not easy to attribute to any known phases.

Fig. 5 shows ^{27}Al MAS NMR spectra of the glass before annealing and spectra of samples annealed for 20 h at temperatures in the

Table 1
Percentage of the total fluorine incorporated in BaF_2 as determined from ^{19}F NMR spectra from the resonance at −16 ppm (error ± 2%).

Annealing temperature in °C	Fluorine in the crystal phase in wt%
500	35
520	47
540	49
580	46
600	44

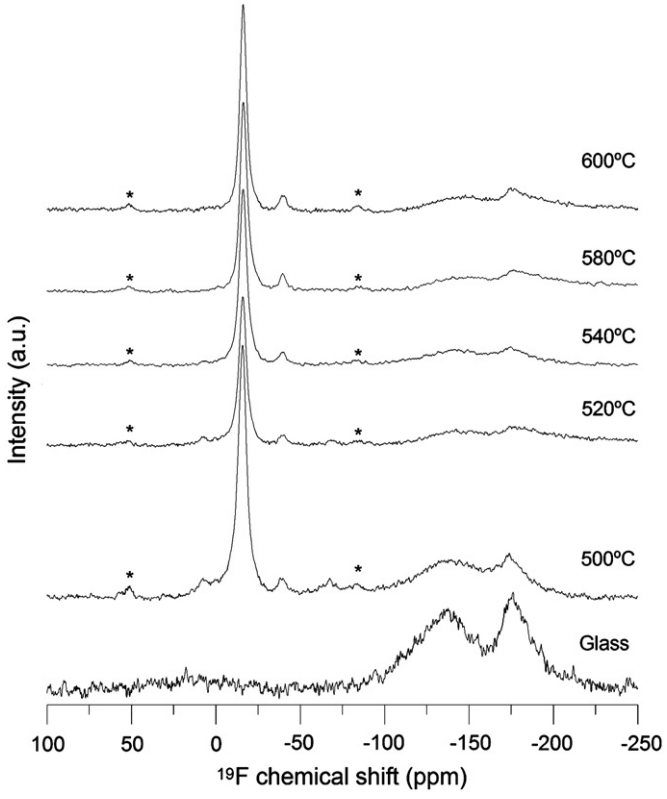

Fig. 4. ^{19}FMAS NMR spectra of samples containing 6 mol% BaF_2 without annealing and annealed at temperatures from 500 to 600 °C for 20 h. The asterisks refer to the spinning side bands.

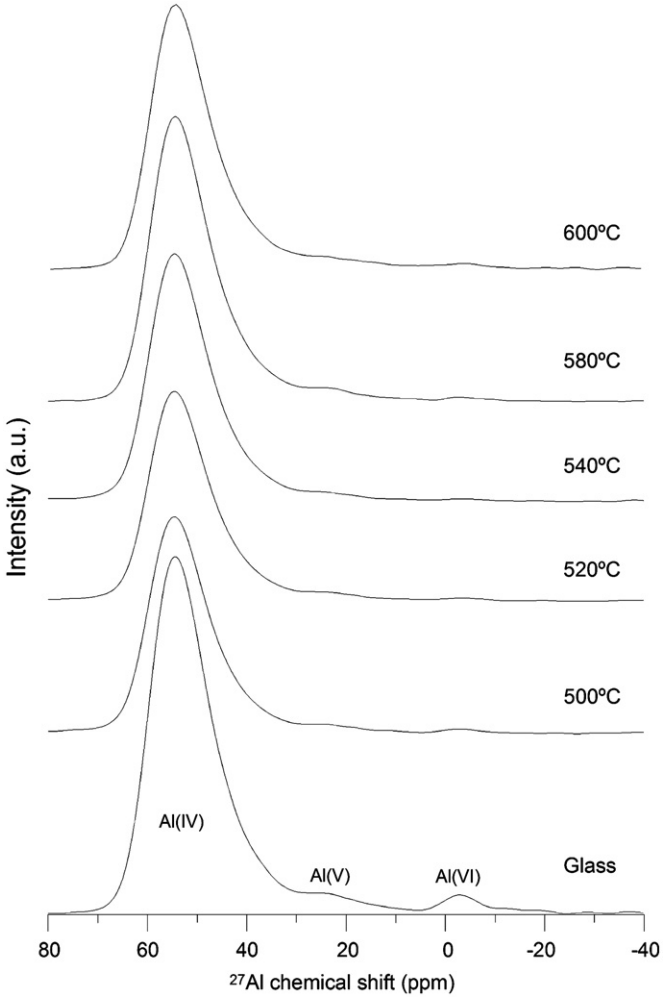

Fig. 5. ^{27}Al MAS NMR spectra of samples containing 6 mol% BaF_2 without annealing and annealed at temperatures from 500 to 600 °C for 20 h. The asterisks refer to the spinning side bands.

range 500–600 °C. The spectrum of the glass sample shows a main resonance band at 60 ppm and two other small ones at 30 and −5 ppm, which are assigned to aluminium in four-, five- and six-fold coordinations, respectively [24]. However, the spectra of the glass-ceramic samples present the main resonance attributed to Al(IV) species with negligible contributions of Al(V) and Al(VI) species.

Fig. 6 depicts the ^{27}Al MAS NMR spectra of glasses containing different BaF_2 concentrations, from 0 to 6 mol% BaF_2. It can be seen that the concentrations of Al(V) and Al(VI) species increase with an increasing BaF_2 concentration in glasses.

4. Discussion

Annealed samples show notably broadened XRD-lines, all attributable to crystalline BaF_2 (see Fig. 1). The crystallite sizes of these samples, calculated from the XRD-line broadening using Rietveld-refinement, are in the range 7–15 nm. The fraction of the crystalline phase increases with the annealing time as well as with the temperature (see Figs. 2 and 3). Annealing the samples at 500 °C for 160 h led to the crystallization of approximately 4 wt% BaF_2, while annealing at 540 °C resulted in approximately 6 wt% BaF_2 already after 40 h. Annealing at even higher temperatures and shorter times, i.e. at 600 °C for 20 h, led to the precipitation of about 5 wt% BaF_2. Assuming a relative fluorine loss of 34% during melting as reported from the previous studies [12], the fluorine concentration in the glass is still attributed to 9 wt% BaF_2. Hence, if after annealing, 5 wt% BaF_2 are crystallized, approximately (54 ± 5)% of fluorine atoms are incorporated in the crystalline phase. This estimation is in agreement to the calculations from NMR spectra (see Table 1).

The volume fraction φ of crystalline BaF_2 can be calculated using Eq. (1)

$$\varphi = \frac{V_C}{V_C + V_{RG}} = \frac{\rho_{RG}}{\rho_{RG} + \frac{\rho_C}{c_C} - \rho_C}, \quad (1)$$

with c_C as the concentration of crystalline phase in wt%, V_C and V_{RG} as the volume fraction and ρ_C and ρ_{RG} are the densities of the crystalline and the residual glassy phase, respectively. The density of the cubic BaF_2 was reported to be $\rho_C = 4.89\ \mathrm{g\,cm^{-3}}$ [25] and for the residual glassy phase a density of $\rho_{RG} = 2.4\ \mathrm{g\,cm^{-3}}$ is assumed (measured from a glass with approximately the same composition, i.e. a smaller BaF_2 concentration and additional BaO in agreement with the assumed fluorine loss). Using the volume fraction and the mean size of the crystallites d (obtained from the line broadening in the XRD, using Rietveld-refinement), the number of crystals N in a certain volume V can be calculated by Eq. (2)

$$N = \frac{\varphi V}{V_C} = \frac{6\varphi V}{\pi d^3}, \quad (2)$$

with V_C as the volume of the crystal which is assumed to possess a spherical shape.

In Fig. 7, the number of crystals (per volume) as a function of annealing time and temperature is shown. The error bars were

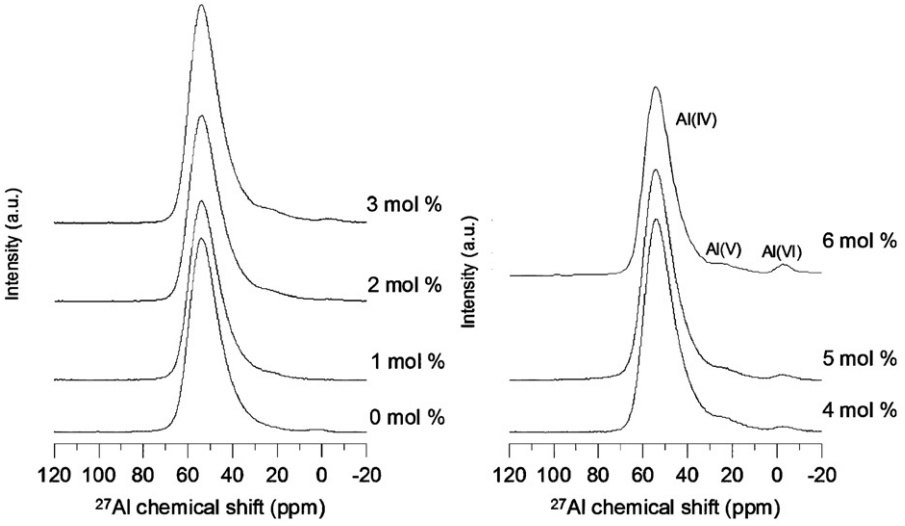

Fig. 6. ^{27}Al MAS NMR spectra of glasses with different BaF_2 concentrations in the range 0–6 mol%. The asterisks refer to the spinning side bands.

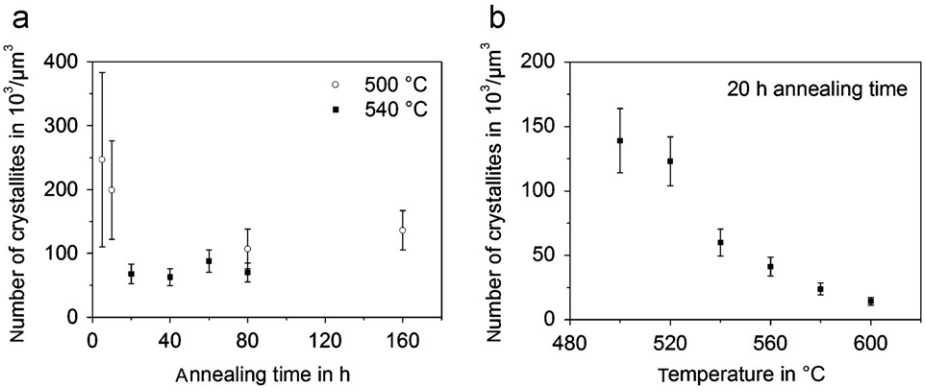

Fig. 7. Number of BaF_2 crystallites as a function of (a) annealing time and (b) temperature in the sample with 6 mol% BaF_2.

calculated according to Eq. (3)

$$\Delta N = \left|\frac{\partial N}{\partial \varphi}\right| \Delta\varphi + \left|\frac{\partial N}{\partial d}\right| \Delta d \quad (3)$$

The absolute error $\Delta\varphi$ was calculated from Eq. (1), where error values are attributed to the crystalline fraction c_C and the density of the residual glassy phase ρ_{RG}.

There is no change in the number of crystals (within the limits of error) with an increasing annealing time as shown in Fig. 7a. This indicates that no coarsening by Ostwald ripening or coalescence occurs. In Ref. [12], these findings are discussed by the very narrow crystallite size distributions in the glass-ceramics. It should be noted that annealing the samples at 500 °C for 5 and 10 h resulted in large error bars. This is due to the small crystallite sizes and the small crystallite fraction, which are close to the detection limit of an XRD. Both errors are included in the error calculation of Eq. (3). However, a notable decrease in the number of crystals is observed with an increasing annealing temperature from $150 \times 10^3\ \mu m^{-3}$ at 500 °C to $14 \times 10^3\ \mu m^{-3}$ at 600 °C, as shown in Fig. 7b. According to Tammann [26], a one step annealing process leads to different nucleation rates at different temperatures. During annealing at temperatures larger than that attributed to the maximum nucleation rate, the number of crystals in the glass-ceramics should decrease (see Fig. 7b). Simultaneously, the crystal growth velocity increases and hence the crystal size at constant annealing time and different temperatures should increase [11]. Recent studies on the crystal growth using Monte Carlo simulation and taking into account the kinetics and development of stresses during crystallization led to the conclusion that the crystal growth rate is decelerated with an ongoing time in this type of glass systems [27].

The glassy network is described according to Zachariasen in Ref. [28] as a random distribution of network forming (NF) and network modifying (NM) components. It is assumed, that NFs, such as SiO_2, B_2O_3 or P_2O_5, form covalent bonds and NMs, such as Na_2O, K_2O, CaO or BaO, are incorporated into the network via ionic bonds. In the glass system under investigation, an SiO_2 is the main NF and K_2O, Na_2O represent the NMs. Since $(([K_2O] \cdot [Na_2O])/[Al_2O_3] > 1)$, Al_2O_3 is mainly incorporated as an NF. The formed AlO_4^- tetrahedra are charge balanced by alkaline or alkaline earth cations. If a coordination number of eight is assumed for Ba^{2+}, it should be surrounded by the two non-bridging oxygens and six bridging oxygens in order to maintain electroneutrality. Of course, this is only an average value, which might locally be different. Concerning the incorporation of F^- into the silicate network, various possibilities are discussed in the literature. In Ref. [29], studies on the structure of fluorine containing soda-lime glasses as well as aluminium silicate glasses are reported. In the alkali glasses, it seems that fluorine prefers to coordinate Na^+ ions, while in calcium containing glasses it can be found close to Ca^+ ions. For glasses which additionally contain aluminium, the fluorine coordinates Al^{3+} ions [16,17,20].

An ^{19}F NMR spectra (see Fig. 5) show that fluorine in glass is mainly involved in Al–F–Ba or Al–F–Na bonds. Nevertheless, it cannot be excluded that a very small amount of F^- is coordinated with silicon, and hence forms SiO_3F-tetrahedra. It can be seen from Fig. 5 that a very small concentration of fluorine is arranged in Ba–F bonds. The coordination of barium with fluorine in an amorphous state can be interpreted as an advantageous structural state to develop BaF_2 crystals during subsequent thermal annealing. As seen in Fig. 4, remarkable difference between the ^{19}F NMR spectra of samples annealed using different annealing temperatures and times are not observed. By contrast, the ^{27}Al MAS NMR spectra are notably different. In the glass sample, small resonances of Al(V) and Al(VI) species are observed. However in the spectra of the glass-ceramics, these resonances are nearly vanished. The detection of these species is very hard due to their higher quadrupolar coupling constant combined with their low intensities. Therefore, nearly all aluminium is four-fold coordinated. Thus, it can be concluded that Al(V) and Al(VI) are mainly present in the glass if fluorine is bonded to aluminium atoms through Al–F–Na or Al–F–Ba bonds. If during thermal annealing, BaF_2 crystallizes, fluorine moves away from these bonds with aluminium and then aluminium turns to occur exclusively in the fourfold coordination in the glass-ceramics, coordinated with oxygen or the remaining fluorine. Hence, during crystallization, the coordination sphere of aluminium in the glassy phase is affected. The ^{27}Al MAS NMR spectra of glasses containing different BaF_2 concentration in Fig. 6 show the effect of fluorine concentration in glasses on the distribution of aluminium species. With an increasing BaF_2 concentration in the glass, the amount of Al(V) and Al(VI) species also increases.

These findings are in agreement to the results of Stamboulis et al. and Karpukhina et al. [18,30] in calcium–alumosilicate glasses. Also in this glass system, fluorine is preferably bonded to the alkaline-earth ion Ca^{2+} as Ca–F or Al–F–Ca bonds, while Si–F–Ca bonds were not proved. In Ref. [20], it is reported that NMs such as M^{2+} (M=Ba, Ca, Mg) are attracting more fluorine with an increasing field strength of the ion, i.e. are competing more effectively with Al^{3+} in order to form metal fluorine bonds. The strong effect of the fluorine concentration on the glass properties such as viscosity or glass transformation temperature (T_g) is discussed by Hill et al. [31]. It is assumed that a complex of CaF^+ is formed which acts in an analogy to alkali ions, and hence affects the depolymerisation of the glassy network stronger than Ca^{2+}. It can be assumed that the latter builds up bridges between two non-bridging oxygen. Also in the case of the BaF_2 glass system, the viscosity decreases rapidly and non-linear with the addition of fluorine [14].

5. Conclusion

During annealing glasses in the system $Na_2O/K_2O/Al_2O_3/SiO_2/BaF_2$, crystallization of cubic BaF_2 is observed. The crystallites formed are smaller than 20 nm as shown by the X-ray diffraction. Furthermore, Rietveld-refinement was used to quantify the crystalline BaF_2 fraction in the glass-ceramics. With increasing annealing times, the concentration of crystalline BaF_2 increases until a saturation is reached at approximately 5–6 wt%. The higher the annealing temperature, the faster the limiting value is reached. The number of crystallites decreases with an annealing temperature, while it remains constant within the limits of error when the annealing time is varied. The latter proves that Ostwald ripening does not occur.

The role of fluorine in the glassy network is studied by an MAS NMR spectroscopy. Here, glasses with different fluorine concentrations and crystallized samples were investigated. In the glassy network, the incorporation of fluorine in Al–F–Ba, Al–F–Na and Ba–F bonds and also the formation of BaF^+ complex is most probable. During annealing the glasses, Ba–F bonds transform into crystalline BaF_2, which is proved by ^{19}F MAS NMR spectra. Aluminium with coordination numbers >4 (Al(V,VI) species) disappears after thermal annealing of the glass. This is due to the transformation of Al(V,VI)-F–Ba into BaF_2, thus increasing the relative proportion of Al(IV) tetrahedra in the crystallized samples.

Acknowledgment

This work was funded by the European community within the Strep project INTERCONY (NMP3-CT-2006-033200).

References

[1] X. Qiao, Q. Luo, X. Fan, M. Wang, J. Rare Earths 26 (2008) 883–888.
[2] X. Qiao, X. Fan, M. Wang, Scr. Mater. 55 (2006) 211–214.
[3] Y. Dwivedi, S.B. Rai, Opt. Mater. 31 (2008) 87–93.
[4] Y. Yu, D. Chen, Y. Wang, F. Liu, E. Ma, J. Non-Cryst. Solids 353 (2007) 405–409.
[5] D. Chen, Y. Wang, Y. Yu, E. Ma, Z. Hu, J. Phys. Condens. Matter 17 (2005) 6545.
[6] D.N. Patel, R.B. Reddy, S.K. Nash-Stevenson, Appl. Opt. 37 (1998) 7805–7808.
[7] Y. Kawamoto, R. Kanno, J. Qiu, J. Mater. Sci. 33 (1998) 63–67.
[8] S. Tanabe, H. Hayashi, T. Hanada, N. Onodera, Opt. Mater. 19 (2002) 343–349.
[9] R.P.F. de Almeida, C. Bocker, C. Rüssel, Chem. Mater. 20 (2008) 5916–5921.
[10] C. Rüssel, Chem. Mater. 17 (2005) 5843–5847.
[11] C. Bocker, C. Rüssel, J. Eur. Ceram. Soc. 29 (2009) 1221–1225.
[12] C. Bocker, S. Bhattacharyya, T. Höche, C. Rüssel, Acta Materialia 57 (2009) 5956–5963.
[13] S. Bhattacharyya, C. Bocker, T. Heil, J.R. Jinschek, T. Höche, C. Rüssel, H. Kohl, Nano Lett. 9 (2009) 2493–2496.
[14] C. Bocker, I. Avramov, C. Rüssel, Chem. Phys. 369 (2010) 96–100.
[15] R.G. Hill, A. Stamboulis, R.V. Law, J. Dent. 34 (2006) 525–532.
[16] T.J. Kiczenski, J.F. Stebbins, J. Non-Cryst. Solids 306 (2002) 160–168.
[17] Q. Zeng, J.F. Stebbins, Am. Mineral. 85 (2000) 863–867.
[18] A. Stamboulis, R.G. Hill, R.V. Law, J. Non-Cryst. Solids 333 (2004) 101–107.
[19] J.F. Stebbins, Q. Zeng, J. Non-Cryst. Solids 262 (2000) 1–5.
[20] T.J. Kiczenski, L.-S. Du, J.F. Stebbins, J. Non-Cryst. Solids 337 (2004) 142–149.
[21] G. Pietzka, P. Ehrlich, Angew. Chem. 65 (1953) 131–135.
[22] L.S. Zevin, G. Kimmel, Quantitative X-ray Diffractometry, Springer, New York, Berlin, 1995.
[23] D. Massiot, F. Fayon, M. Capron, I. King, S. Le Calvé, B. Alonso, J.-O. Durand, B. Bujoli, Z. Gan, G. Hoatson, Magn. Reson. Chem. 40 (2002) 70–76.
[24] D.R. Neuville, L. Cormier, D. Massiot, Chem. Geol. 229 (2006) 173–185.
[25] A.S. Radtke, G.E. Brown, Am. Mineral. 59 (1974) 885–888.
[26] G. Tammann, Der Glaszustand, Voss, Leipzig, 1933.
[27] N. Tsakiris, P. Argyrakis, I. Avramov, C. Bocker, C. Rüssel, Europhys. Lett. 89 (2010) 18004.
[28] W.H. Zachariasen, J. Am. Chem. Soc. 54 (1932) 3841–3851.
[29] J.F. Stebbins, S. Kroeker, S. Keun Lee, T.J. Kiczenski, J. Non-Cryst. Solids 275 (2000) 1–6.
[30] N. Karpukhina, R.V. Law, R.G. Hill, Adv. Mater. Res. 39–40 (2008) 25–30.
[31] R.G. Hill, N.D. Costa, R.V. Law, J. Non-Cryst. Solids 351 (2005) 69–74.